Impact of interstitial iron on the study of meta-stable B-O defects in Czochralski silicon: Further evidence of a single defect

Moonyong Kim,[1,a)] Daniel Chen,[1] Malcolm Abbott,[1] Nitin Nampalli,[1] Stuart Wenham,[1] Bruno Stefani,[1,2] and Brett Hallam[1]
[1]*School of Photovoltaic and Renewable Energy Engineering, University of New South Wales, Sydney, NSW 2052, Australia*
[2]*School of Engineering, Federal University of Rio Grande do Sul, Porto Alegre, Brazil*

(Received 15 August 2017; accepted 17 January 2018; published online 6 February 2018)

We explore the influence of interstitial iron (Fe_i) on lifetime spectroscopy of boron-oxygen (B-O) related degradation in p-type Czochralski silicon. Theoretical and experimental evidence presented in this study indicate that iron-boron pair (Fe-B) related reactions could have influenced several key experimental results used to derive theories on the fundamental properties of the B-O defect. Firstly, the presence of Fe_i can account for higher apparent capture cross-section ratios (k) of approximately 100 observed in previous studies during early stages of B-O related degradation. Secondly, the association of Fe-B pairs can explain the initial stage of a two-stage recovery of carrier lifetime with dark annealing after partial degradation. Thirdly, Fe_i can result in high apparent k values after the permanent deactivation of B-O defects. Subsequently, we show that a single k value can describe the recombination properties associated with B-O defects throughout degradation, that the recovery during dark annealing occurs with a single-stage, and both the fast- and slow-stage B-O related degradation can be permanently deactivated during illuminated annealing. Accounting for the recombination activity of Fe_i provides further evidence that the B-O defect is a single defect, rather than two separate defects normally attributed to fast-forming recombination centers and slow-forming recombination centers. Implications of this finding for the nature of the B-O defect are also discussed. *Published by AIP Publishing.* https://doi.org/10.1063/1.5000323

I. INTRODUCTION

Light-, or more specifically, carrier-induced boron-oxygen (B-O) related degradation in Czochralski silicon wafers has been widely studied over decades.[1–5] However, there is still significant debate going on about the structure and properties of the B-O defect.[6–9] One particularly well-understood behaviour of B-O related degradation is that the reduction of minority carrier lifetime occurs in two stages. In *p*-type silicon, it proceeds with a fast, but generally, small degradation of the carrier lifetime with a timescale of approximately 100 s, followed by a much slower, and larger degradation of the carrier lifetime that occurs over approximately 48 h.[10,11] A similar two-stage degradation can also be observed in compensated *n*-type silicon albeit at slower time-scales.[12–15]

However, the nature of two-stage degradation has been a contentious issue. There is a continuing debate about whether the fast and slow degradation are caused by two separate defects[11,16] or a single defect.[9,17,18] In early studies, it was proposed that the degradation was caused by two distinctively different B-O related defects, due to the differing time constants of degradation.[11,19] A key argument presented by Bothe and Schmidt for the existence of two separate defects was the determination of different capture cross-section ratios (k) of 100 and 10, for the fast and slow stages of degradation, respectively, assuming one single-level defect centre for each stage of degradation.[11] The same paper also presented the second argument in favour of the two-defect hypothesis, based on different behaviours observed for the recovery of carrier lifetime with dark annealing (DA) after fast or slow degradation. Dark annealing after only the fast degradation stage led to a two-stage lifetime recovery, whereas dark annealing after complete degradation led to only a single stage of lifetime recovery. This difference was attributed to two independently forming defect centres. Around the same time, there was a debate about the composition of the recombination centres. While it was clear that degradation was not related to the association of O_{2i} and B_i/B_s, but rather to a configurational change of some complex of B and O, it was not clear whether the form of boron was B_i or B_s. Within this context, the idea of multiple meta-stable defect centres seemed plausible, which led to the use of the terms "fast-forming recombination center" (FRC) and "slow-forming recombination center" (SRC), to describe the degradation in the fast and slow timescales, respectively.[11] This understanding has been used to derive multiple subsequent theories on B-O related degradation.[8,16,19–21]

Subsequent studies showed that recombination of the B-O defects in *n*- and *p*-type silicon was more accurately described by a two-level Shockley-Read-Hall (SRH) defect with a donor level ($E_{B\text{-}O,d}$) and an acceptor level ($E_{B\text{-}O,a}$) for both the SRC ($E_{t,SRC,2d}$ and $E_{t,SRC,2a}$) and the FRC ($E_{t,FRC,2d}$ and $E_{t,FRC,2a}$),[22] rather than a single donor level alone of 0.41 eV for the FRC ($E_{t,FRC,1d}$) and 0.35–0.85 eV for the SRC ($E_{t,SRC,1d}$) respectively.[11]

a)Author to whom correspondence should be addressed: moonyong.kim@unsw.edu.au

More recently, the recombination properties after the permanent deactivation of B-O defects have been investigated.[21] In that study, recombination with a high k-value of 65 was observed after the permanent deactivation process, consistent with the recombination properties of that attributed to the FRC.[16] Hence, it was concluded that only the degradation occurring in the slow timescale could be eliminated during the illuminated annealing processes.

In contrast to many theories suggesting the involvement of two separate defects, it was recently proposed that the fast and slow B-O related degradation could be caused by a single defect.[9] This was based on the measurement of identical recombination properties for fast and slow degradation with a capture cross-section ratio of 19, and the ability to describe multi-stage degradation using a single defect.[9,18] In a subsequent study by Niewelt *et al.*, a revised single-defect parameterisation was presented with a k-value of 18 for the donor level that was able to describe both fast and slow degradation on multiple samples.[23] It should be noted that the difference in the donor-level k-value from earlier work (where it was typically $\approx$10) was due to the fact that Bothe *et al.* assumed a single-level defect, while in more recent studies by Hallam *et al.* and Niewelt *et al.*, the two-level properties of B-O defects were included,[8,9,12,18] as well as the different assumptions used in modelling.[24]

Subsequently, Kim *et al.* demonstrated that the relative ratio of fast and slow degradation could also be modulated by applying short dark annealing processes on pre-degraded wafers.[17] The difference in the ratio not only made no significant difference in k, but the reaction was fully reversible, allowing any ratio of fast and slow degradation to be demonstrated on the same substrate. This provided strong experimental evidence of a close link between the degradation in the fast and slow timescales. It was concluded that in all cases, the degradation attributed to B-O defects is from the same defect rather than from the two independent defects.

However, there remain a number of experimental results in the literature, which cannot be explained by the proposed single defect hypothesis. In particular, the cause of the high apparent k-value during early stages of degradation in the early studies,[11,16,19] differences in the dark annealing kinetics,[11] and the presence of recombination with a high k-value after permanent deactivation remains uncertain.[21] In our previous work, we eluded to the possible influence of interstitial iron in previous B-O related studies[17] due to its known behaviour in boron-doped silicon.[25] We also showed that the typical lifetime subtraction techniques used to investigate B-O defects can lead to an abnormally high k-value in the presence of Fe_i.[18] In this study, the impact of the recombination properties of interstitial iron, and the kinetics of iron-boron pair association and dissociation are investigated in more detail to determine the influence of iron on B-O defect studies.

Iron is a common impurity in p-type Cz silicon that is also influenced by carrier-injection. In the interstitial form, iron (Fe_i) can associate with substitutional boron (B_s) to form Fe-B pairs. This typically occurs at room temperature in the dark. However, these Fe-B pairs can be readily dissociated by illumination, carrier injection, or an applied bias.[26,27] A peculiar behaviour of Fe_i is that a characteristic 'cross-over' point occurs in the injection level-dependent minority carrier lifetime curves when comparing that in the Fe-B and Fe_i states.[28] This is due to the low k-value of Fe-B related recombination and the high k-value of Fe_i related recombination.[25,28] The cross-over point depends on the background doping density of the material, but is typically around $2 \times 10^{14}/cm^3$. For injection levels above the cross-over point, the lifetime is increased in the Fe_i state and is decreased for injection levels below the cross-over point. In contrast, as B-O defects form, the lifetime at all injection levels decreases. However, this effect is more pronounced at low-injection levels due to the stronger influence of the asymmetric Shockley-Read-Hall (SRH) recombination. Furthermore, surface/emitter related recombination is increased with increasing carrier concentration.

In this paper, we provide a detailed study on the impact of Fe_i and its recombination properties on B-O related degradation studies. We show that several key results from the literature can be explained by the presence of iron:[11,16,21]

1. A higher apparent capture cross-section ratio (k_{app}) of B-O related recombination that occurs in the early stages of degradation.
2. The two-stage recovery of carrier lifetime during dark annealing after early stages of degradation (attributed to the FRC).
3. Recombination activity with a high k-value remaining after permanent deactivation of the B-O defects.

These findings provide further evidence to support the hypothesis that B-O related degradation in p-type Czochralski silicon is due to a single defect rather than two separate defects (FRC and SRC). Furthermore, they demonstrate the importance of accounting for iron when studying meta-stable defects in boron-doped silicon. Finally, the implications of a single defect theory for the nature of the B-O defect are discussed.

II. EXPERIMENTAL METHODS

Symmetrical lifetime test structures and screen-printed solar cells were fabricated on p-type 156 mm × 156 mm mono-crystalline solar-grade wafers sourced from LONGi Silicon Materials Corporation, with a measured resistivity of 1.6 Ω cm and initial iron concentrations between $10^{11}/cm^3$ and $10^{12}/cm^3$. The wafers were alkaline textured resulting in the removal of 10 μm from each side of the wafer. Half of the samples were pre-gettered by heavy $POCl_3$ diffusion (40 Ω/sq). Subsequently, all wafers were re-textured in an alkaline solution to etch 2 μm from each side of the wafer to remove the getter-diffusion and ensure the same thickness of wafers for the non-gettered samples. The wafers were again $POCl_3$ diffused with either a heavy (60 Ω/sq)[29] or a lightly diffused emitter recipe (120 Ω/sq).[30] The heavily diffused wafers were also annealed at 650 °C for 12 h (LTA), which is a known method to reduce interstitial iron concentration by precipitation of the iron.[31] The annealing condition used may vary the equilibrium condition of B-O defects. However, this should not affect the B-O related reaction rates. The lightly diffused

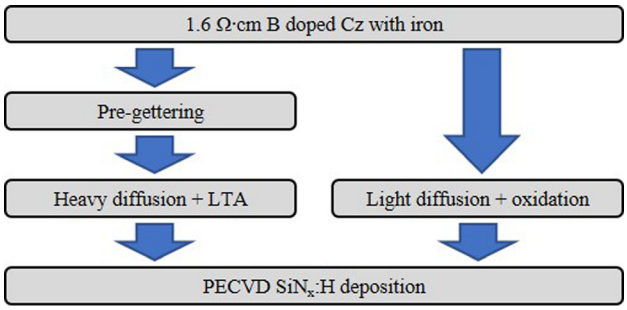

FIG. 1. Schematics of experimental details.

wafers were oxidised at 800 °C for 15 min to increase the dissolution of precipitated iron from the bulk.[32–34] Silicon nitride with a refractive index of 2.08 at 633 nm was deposited using plasma-enhanced chemical vapour deposition (PECVD) on both sides of all samples to form symmetric lifetime test structures.[35] Figure 1 summarises the process flow. Each wafer was then cleaved using a laser into 52 mm × 52 mm tokens.

The samples were annealed and light soaked at various temperatures for various times (Table I) to either modulate the fast- and slow- degradation, dissociate, form or passivate B-O defects. Either LS_3 and LS_4 was done after resting in the dark for 24 h to show the effect of iron after full iron dissociation.

All samples were dark annealed at 200 °C for 10 min to dissociate any pre-formed B-O defect during processing.[11] The samples were left in the dark for more than 24 h to ensure complete association of Fe-B pairs, which can be induced during the dark annealing at high temperature.[36] Samples were characterised using quasi-steady-state photoconductance (QSS-PC) lifetime measurements.[37] The measured data were analysed using a generalised method[38] and corrected for Auger and radiative recombination.[39] The interstitial iron concentration was extracted from the difference in the effective lifetime at $\Delta n = 1 \times 10^{15}/\text{cm}^3$ before and after approximately 5–10 s of illumination under halogen lights with an intensity equivalent to ≈1 sun.[40] For the given samples, it was sufficient to dissociate >99% of Fe-B pairs. We confirmed this by observing no changes in the lifetime with additional light soaking (LS) for a few seconds. This was also theoretically confirmed with the known dissociation rate at a given light intensity and iron concentration where under 5–10 s of exposure, Fe-B that remained is expected to be <1%.[26] Furthermore, the difference in the interstitial iron concentration after 5 s or 10 s of illumination is expected to be less than 1%.

TABLE I. Dark annealing (DA) and light soaking (LS) process duration, light intensity and temperature.

Condition	T (°C)	t	Light intensity (sun) (if applicable)
DA_1	200	15 s	…
DA_2	200	600 s	…
DA_3	250	1 h	…
LS_1	25	48 h	0.2
LS_2	25	300 s	0.2
LS_3	25	5 s	1
LS_4	25	10 s	1
PD	160	2 h	1

Degradation was performed at 25 °C with a constant illumination intensity of 0.02 sun to study the influence of interstitial iron on B-O defect formation. *In-situ* lifetime measurements at room temperature were obtained using the Sinton Instruments WCT-120 lifetime tester, analysed using the generalised technique[38] and corrected for the bias light. The *k*-value for the donor level of the B-O defect was analysed using the carrier lifetime model described by Nampalli *et al.*,[24] assuming a single-level defect.

For the B-O defect dissociation study, samples were dark annealed at 200 °C for 10 min followed by partial degradation at 30 °C under 0.2 sun illumination for 600 s. The annihilation rate of B-O defects was analysed by taking *in-situ* lifetime measurements of samples with and without the presence of iron using the Sinton Instruments WCT-120TS tool at a temperature of 375 K. Before any of the *in-situ* measurements, the samples were light soaked under 1 sun for approximately 5 s to deliberately dissociate Fe-B pairs that are present in the wafers. The Dorkel/Leturcq model[41,42] was used for the mobility modelling for elevated temperature measurements.

In order to investigate the permanent deactivation of fast and slow B-O related degradation, lifetime samples were fired at a set peak temperature of 700 °C (596 ± 5 °C of actual wafer temperature) in a belt furnace and annealed at 250 °C for 1 h to destabilise any potentially passivated B-O defects during the firing.[43] As demonstrated by Walter *et al.*, this process would not significantly impact the equilibrium concentration of B-O defects.[44] These were then light soaked under 0.2 sun at 25 °C for 48 h to fully degrade the samples (LS_1). The samples were then annealed at 200 °C either for 15 s or for 600 s (DA_1 or DA_2) to modulate the extent of fast and slow degradation, as previously demonstrated.[17] All samples were then subjected to complete degradation (LS_1), followed by illuminated annealing at elevated temperatures (160 °C under 1 sun for 2 h), to passivate B-O defects. The stability of the permanent deactivation by the hydrogen passivation was checked by a subsequent light soaking process with an illumination intensity of 0.2 sun for 48 h at 30 °C. The normalised defect density, $NDD(t)$, during light soaking was calculated as

$$NDD(t) = \frac{1}{\tau(t)} - \frac{1}{\tau_{DA}},$$

where $\tau(t)$ is the lifetime after light soaking for time t and τ_{DA} is the lifetime after 10 min of dark annealing at 200 °C. To ensure there is no influence of lifetime by dissociated iron, the lifetime was measured after keeping the sample in the dark for at least 3 h, which is the minimum time required to associate >99% of iron with known temperature and background doping density.[45] The error due to incomplete association of iron, for example, >5% will be less than 1 μs. Following this, the normalised defect density (*NDD*) can be translated into a fractional defect density (*FDD*), using the following equation:

$$FDD = \frac{NDD(t)}{NDD_{full}},$$

where NDD_{full} is NDD after 48 h of light soaking for full degradation. NDD_{fast}, which is the NDD due to fast degradation, is determined after 300 s of light soaking.

III. RESULTS AND DISCUSSION

A. Impact of Fe_i on the apparent capture cross-section ratio throughout B-O degradation

Fe_i has significant impact on the recombination properties of the silicon material and, particularly, on the apparent capture cross-section ratio (k_{app}) of B-O defects. *In-situ* measurements with constant light soaking were analysed to extract the k_{app} throughout degradation, as shown in Fig. 2. From the experimental data, k_{app} was determined based on fitting the lifetime data to a model that accounted for the recombination of intrinsic effects (Auger and radiative recombination), the surface/emitter and background bulk SRH defects (other than B-O and Fe_i) using the method D presented by Nampalli *et al.*[24] For fitting, the lifetime curves were separated into components of dark saturation current density, J_{0e}, bulk lifetime, τ_{bulk}, and SRH lifetime. The J_{0e} and τ_{bulk} of the samples were allowed to float, with resultant values of $J_{0e} = 40 \pm 13$ fA/cm^2 and $\tau_{bulk} = 111 \pm 34\,\mu$s. SRH recombination was assumed to be caused by a single defect with a trap energy level of $E_t = 0.41$ eV below the conduction band. Curve fitting was performed by minimizing the sum of squared residual terms using a quasi-Newton nonlinear regression algorithm. A goodness of fit was established to determine a reduced Chi-squared metric (χ^2). For further details, see Ref. 24.

This paper has attempted to explain the observed experimental results with the assumption that only interstitial iron and meta-stable boron-oxygen defects were formed via the light soaking and annealing steps. This assumption is well founded, given the ability of the known kinetics of those defects to fit all of the trends and the lifetime fitting procedures to have not detected any significant influence of other recombination sources. However, it should be acknowledged that there are many other possible known and unknown meta-stable defects within silicon wafers, and the influence of these cannot be ruled out completely. However, the observations are unlikely copper-LID due to a differing k-value with a different time scale of degradation.[46,47] Furthermore, oxygen precipitates, which are a common defect in Cz silicon, are unlikely to have influenced the results, as they are not known to be light induced. With recombination from sources other than B-O and Fe accounted for, k_{app} was then determined by attributing the remaining recombination lifetime, τ_{app}, to a single SRH defect. Although we recently discovered that the LeTID can also be formed in the dark in mono.[48] However, as the peak firing temperature was done at a set temperature of 700 °C, which is the wafer temperature of 596 °C, where no LeTID in the dark or under illumination is expected to occur that may influence the results of this study. Furthermore, light soaking was performed at room temperature with low intensity, where the LeTID is not expected to occur. Thus, the apparent lifetime τ_{app} was only based on the lifetime of B-O defects, $\tau_{B\text{-}O}$, Fe_i, τ_{Fei}, or Fe-B, $\tau_{Fe\text{-}B}$ as follows:

$$\frac{1}{\tau_{app}(t)} = \frac{1}{\tau_{B-O}(t)} + \frac{1}{\tau_{Fe_i}(t)} + \frac{1}{\tau_{Fe-B}(t)},$$

where t is the light soaking time.

Both the energy level reported by Bothe and Schmidt with a one-level defect[11] and the energy levels reported by Hallam *et al.* with a two-level defect[18] were used to analyse the k-value on samples with and without iron. As is seen in Fig. 3, on the sample with an undetectable amount of iron ($[Fe_i] < 1 \times 10^9$/cm^3), a k-value of ≈10 (for a single-level) or ≈18 (for two-levels) was obtained throughout the duration of light soaking, which compare well with the expected k-values of the B-O defect.[11,18] The large errors observed in the first 1000 s of the measurement are due to the small

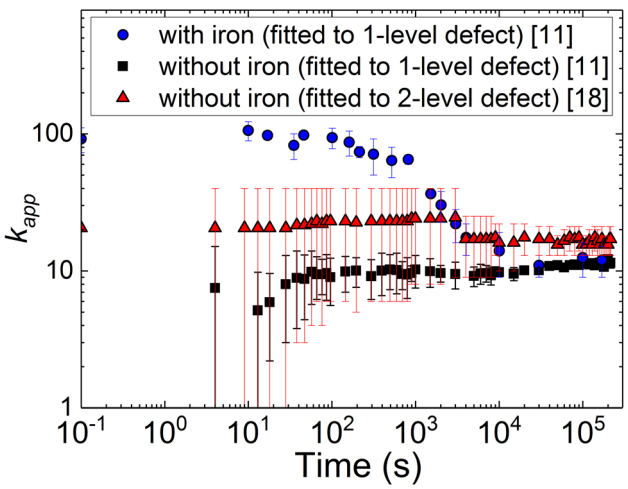

FIG. 2. Apparent capture cross-section ratio (k_{app}) that was fitted to either a single-level defect of SRC[11] or a two-level defect[18] during light soaking with 0.02 sun at room temperature using *in-situ* QSS-PC lifetime measurements, with iron ($[Fe_i] = 2.6 \pm 0.5 \times 10^{11}$/cm^3) and with an undetectable iron concentration ($[Fe_i] < 1 \times 10^9$/cm^3).

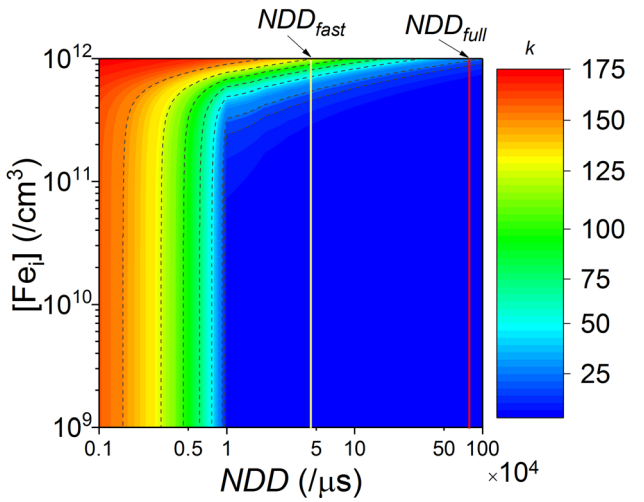

FIG. 3. Contour plot of the theoretical apparent capture cross-section ratio (k_{app}), as a function of the interstitial iron concentration [Fe_i] and the normalised defect density of boron-oxygen (B-O) defects (NDD). The typical NDD from fast degradation (NDD_{fast}) is shown in the yellow line and the NDD after full degradation (NDD_{full}) is shown in the red line.

signal to noise ratio during the early stages of degradation. However, the fits with minimised χ^2 (below 1) consistently displayed a capture cross-section ratio below 20 assuming a single defect level. In contrast, the sample with iron ($[Fe_i] = 2.6 \pm 0.5 \times 10^{11}/cm^3$) displayed a much higher initial k_{app} of approximately 100 when it was fitted with $E_{t,SRC,1d}$, which is within the range of the k-value reported for the FRC by Bothe *et al.*[11] The k-values extracted from the iron-contaminated sample gradually decreased after 1000 s and converged to a k-value of 10 with a single-level defect approximation as the B-O related degradation began to dominate. It should be noted that the degradation was performed under 0.02 sun, which was a much lower intensity than the illumination used to deliberately dissociate Fe-B pairs prior to the *in-situ* measurements. Given that the dissociation rate of Fe-B depends on the illumination intensity, a new equilibrium between Fe_i and Fe-B is established influencing the k_{app}.

Simulations were performed to further demonstrate the impact of interstitial iron on the extracted recombination properties of B-O defects for a range of $[Fe_i]$. The modelling considered the recombination properties of both B-O defects and Fe_i, to create theoretical injection-level dependent Shockley-Read-Hall (SRH) related lifetime curves. A background doping density of $1 \times 10^{16}/cm^3$ and a wafer thickness of 180 μm were used (as typical values for p-type solar cells). However, the specific values chosen do not alter the key conclusions drawn from the simulations. For B-O defects, a recent parameterisation for the two-level defect was used,[18,49] with a k-value for the donor level of $k_{B\text{-}O} = 18$. For Fe_i, all iron was assumed to be dissociated from boron, with $k_{Fei} = 286$, which is based on the reported capture cross-section values of electrons and holes of interstitial iron.[28]

A parameterisation method was used for the SRH lifetime approximation using the normalised defect density (NDD).[50] An apparent capture cross-section ratio (k_{app}) of SRH recombination was then obtained assuming a single defect. Therefore, the SRH lifetime τ_{SRH} was only based on the lifetime of B-O defects, $\tau_{B\text{-}O}$, or that of Fe_i, τ_{Fei}, as follows:

$$\frac{1}{\tau_{SRH}} = \frac{1}{\tau_{B-O}(NDD)} + \frac{1}{\tau_{Fe_i}([Fe_i])},$$

where NDD is the NDD of B-O defects and $[Fe_i]$ is the iron concentration. The k_{app} was then estimated using the ratio of the SRH lifetime τ_{SRH} at two injection levels of $10^{16}/cm^3$ and $10^{12}/cm^3$. The values of NDD after full degradation (NDD_{full}) and after fast degradation ($NDD_{fast} \approx 0.1 \times NDD_{full}$) were estimated using multiple measurements of our identical symmetrical lifetime structure samples with a 65 Ω/sq emitter and SiN_x:H dielectric passivation layers.

The simulated impact of Fe_i and NDD of B-O defects on the k_{app} is shown in Fig. 3. Increasing the $[Fe_i]$ for a given NDD increases the effective k_{app}, whereas increasing the NDD for a given $[Fe_i]$ decreases k_{app}. For the sensitivity analysis, when k_{Fei} varies between 51 and 570, which are the highest and the lowest values of k_{Fei} reported, the k_{app} varies between 25 and 150 with $[Fe_i] = 1 \times 10^{12}/cm^3$ and $NDD = NDD_{fast}$. Although it has a large range of k_{app}, this can nevertheless highlight the influence of iron on the value of k_{app}. This result is not entirely unexpected since the total recombination within the sample comprises the relative combination of both defects. It does, however, highlight that for the concentrations typically found in solar grade Cz silicon, the extraction of k_{app} is only impacted in the early stages of degradation. This behaviour is consistent with the experimental results shown in Fig. 3. This highlights that during early stages of B-O related degradation, in the presence of Fe_i, samples would be expected to have higher apparent k_{app} values. This offers a possible explanation for the higher capture cross-section ratio attributed to the FRC in early studies, and is in agreement with suggestions of a single defect causing both rapid and slow B-O related degradation.[9,17]

It is worth noting that in any given experiment, the actual concentration of Fe_i will depend strongly on the history of the sample. For example, if the sample has been stored in the dark for several hours then, all the Fe_i would bond with boron to form Fe-B pairs. Conversely, any illumination on the sample (including bias lights and flashes used to measure lifetime) will act to dissociate Fe-B pairs, increasing the concentration of Fe_i until it saturates. The bulk doping of the wafers will also have an influence on both the association and dissociation rates, as well as the relative impact on the lifetime curve itself due to the changing SRH properties. Assuming that half of the recovery after fast degradation can be attributed to iron, from the given illumination intensity and cell thickness, an upper limit for the potential iron concentration in the study by Bothe *et al.*[11] is $2.9 \times 10^{11}/cm^3$. This is well within the range of naturally occurring iron concentrations in the wafers used in the present manuscript.

The theoretical and experimental results here provide an alternative explanation for earlier results that measured the relatively high values of k_{app} during early stages of degradation.[11] In that paper, the samples were not phosphorus diffused and hence were not gettered. The samples could, therefore, have contained significant concentrations of iron, although this was not explicitly addressed.[51] Since the time of those studies, there have been great improvements in the ability to measure and interpret effective lifetime curves, particularly, regarding the behaviour of interstitial iron in silicon. Thus, it is possible that the early results previously ascribed to the FRC defect[11] may have been influenced by the presence of $iron_i$.

B. Influence of Fe_i during dark annealing: Possible explanation for different annihilation rates of B-O defect

The NDD is a common parameter in B-O defect studies, used to quantify the concentration of B-O defects at a fixed injection level. However, the NDD calculation has a limitation as it assumes that only a single type of defect changes during processing. Often, this is not the case. In the presence of iron, illumination or dark annealing can cause the

dissociation or association of Fe-B pairs, hence modulating the concentration of Fe_i.[25] This means that in addition to the B-O defects generated during illuminated processes, the concentrations of two separate defects (Fe-B pairs and Fe_i) with very different recombination properties are also modulated by the carrier injection. This can have a significant impact on the apparent *NDD* of B-O defects.

The association kinetics of Fe-B pairs can affect the apparent *NDD* of B-O defects during dark annealing. A simulation was performed where the association rate of Fe-B pairs was compared to the annihilation rate of the FRC reported by Bothe *et al.*[11] to highlight the impact of iron on the apparent annihilation rate of B-O defects. Figure 4 shows experimental data from Bothe *et al.* (symbols) for a two-stage lifetime recovery of the normalised defect concentration, which is essentially the *NDD*.

In the paper by Bothe *et al.*, dark annealing was performed after samples were degraded for 600 s by the applied voltage (to investigate the annihilation of the FRC).[11] Simulations (Fig. 4, lines) represent two simultaneous reactions. The first reaction is for Fe-B pair association based on the known association kinetics at the given temperature for a background doping density of $N_A = 1.5 \times 10^{16}/\text{cm}^3$.[45] This reaction replaced the "fast" stage of recovery in the two-stage recovery described by Bothe *et al.*[11] The second reaction is for B-O defect annihilation, based on the "slow," second stage of the two-stage recovery of carrier lifetime described.[11] The *NDD* was scaled to the results by Bothe *et al.* to directly compare them to the simulation. In this figure, the first half of the *NDD* reduction is assumed to be due to Fe-B pair association, and other half is due to B-O defect annihilation, where reactions start from 1 s. The figure highlights that the known behaviour of Fe-B pairs association can adequately describe most data points for the initial stage of lifetime recovery, and that the conventional annihilation rate of B-O defects can describe the second-stage.

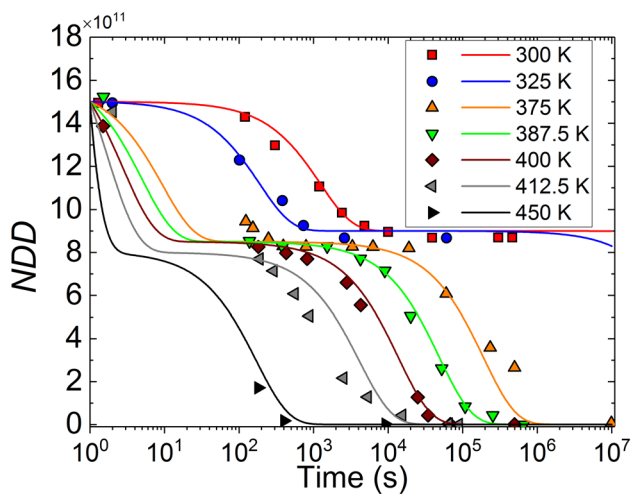

FIG. 4. Normalised defect density (*NDD*) annihilation from data presented by Bothe *et al.* (symbols) using dark annealing under different temperature conditions.[11] Theoretical *NDD* that is based on the activation energy and the attempt frequency of B-O defect annihilation and iron association rate constant with $N_A = 1.5 \times 10^{16}/\text{cm}^3$ is shown in lines.[25]

The reported activation energy of iron association slightly differs from that reported by Bothe *et al.* for the first stage of recovery after fast degradation.[11,45] However, there are also substantial differences in the reported activation energies for various reactions in the B-O defect system.[11,52–56] Furthermore, it is suggested that the activation energies obtained can differ depending on the metric used for the determination.[57] As a result, a deviation in the activation energy may not be sufficient to conclude that observations by Bothe *et al.* were not iron. Furthermore, the reaction rates within the temperature range of 300 K and 325 K lie within expected ranges of Fe-B pair association. The cause for deviations at higher temperatures such as 375 K is unclear. However, there appears to be insufficient data points in the study by Bothe *et al.* to accurately determine the reaction rate for temperatures above 325 K.[58]

To experimentally determine whether Fe-B pair association could have been responsible for this effect, *in-situ* lifetime measurements were taken on samples with and without iron to monitor the apparent *NDD* throughout dark annealing processes when applied to fully degraded samples. Figure 5 shows the *NDD* calculated from the elevated temperature lifetime measurement at 375 K. The effective lifetime measured at 375 K for $\Delta n = 8.0 \times 10^{13}/\text{cm}^3$ was between 28 μs and 48 μs for iron contaminated samples and between 180 μs and 200 μs for iron-free samples. The initial effective lifetime used to determine the apparent *NDD* here is, however, based on the lifetime after 48 h of light soaking and an additional 5 s of light exposure of 1 sun at room temperature. This was to intentionally dissociate iron to demonstrate the influence of iron on the investigation of B-O defects ($LS_1 + LS_3$). Moreover, the additional 5 s of light soaking after 48 h of light soaking should not influence the B-O defects themselves anymore, as B-O defects are already fully formed. For samples with iron, at an injection level $\Delta n = 8.0 \times 10^{13}/\text{cm}^3$, the lifetime showed a rapid recovery. This rapid recovery observed only in the sample with iron in the first 100 s (for $\Delta n_1 = 8.0 \times 10^{13}/\text{cm}^3$) was remarkably similar to that reported in the paper by Bothe *et al.* for the fast recovery after fast degradation.[11] The rate of the first recovery at 375 K, however, was not identical to the recovery rate observed with same temperature by Both *et al.*[11] That could have been due to the difference in the background doping density. Therefore, it is likely an error with reported values for Fe-B association. Using the limited data presented by Bothe *et al.* at 375 K, the time constant can be estimated to be 68/s. Our data at the same temperature gives approximately 46/s where the rate of the two time constant would be approximately 1.5. Considering that the association time constant is inversely proportional to the background doping density,[45] the expected ratio of the association rates with different background doping densities ($1.5 \times 10^{16}/\text{cm}^3$ vs. $9.1 \times 10^{15}/\text{cm}^3$) is 1.65, and hence is in close agreement, given the potential errors in temperature between the different setups. Considering that Bothe *et al.*[11] measured the V_{OC}, which is known to be influenced by the dissociation of Fe-B pairs,[27] at an illumination intensity of 10 mW/cm^2, the injection level at which the cell would operate is below $\Delta n = 1 \times 10^{14}/\text{cm}^3$. This is based on our samples with a

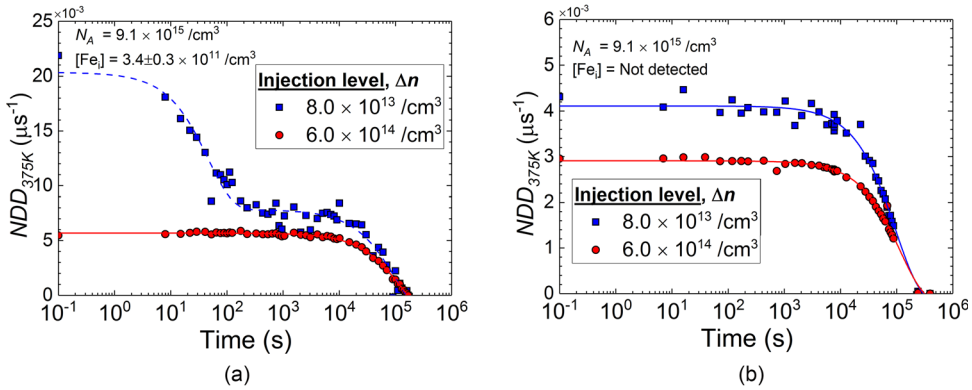

FIG. 5. Normalised defect density at 375 K (NDD_{375K}) of (a) a sample with $[Fe_i] = 3.4 \pm 0.3 \times 10^{11}/cm^3$ and (b) a sample without iron versus dark annealing time at 375 K. NDD_{375K} was based on the lifetimes at two different injection levels ($\Delta n_1 = 8.0 \times 10^{13}/cm^3$ and $\Delta n_2 = 6.0 \times 10^{14}/cm^3$, where Δn_2 is the cross-over point) and was measured at an elevated temperature of 375 K. Solid lines are the single exponential fits and the dashed lines are the two exponential fits.

lifetime of approximately 100 μs at an injection level of $\Delta n = N_A \times 0.1$. This injection level would certainly be below the cross-over point where the dark annealing would cause Fe-B association, and hence the dark annealing would cause an increase in *NDD*.[25,40] As a comparison, when the *NDD* was extracted from $\Delta n = 6.0 \times 10^{14}/cm^3$, which was approximately the cross-over point, only a single recovery was observed. The cross-over point was higher than the typical value of $\Delta n = 2.0 \times 10^{14}/cm^3$, as it was measured at a higher temperature of 375 K.

In contrast, for the sample without iron, regardless of the injection level, only a single stage of lifetime recovery was observed [Fig. 5(b)]. The results are consistent with the presence of iron introducing a first rapid-stage of lifetime recovery if the determination of *NDD* is not performed at the cross-over point. Simulation and experimental results provide an alternative explanation for the first stage of the recovery of "FRC," that was proposed by Bothe *et al.*[11] Furthermore, an identical recovery rate was observed on both fully and partially degraded samples, in both samples free of iron or samples with iron where the lifetime was extracted at the cross-over point.

This suggests that the B-O defects that are formed in the fast and slow timescales are identical, which is in agreement with previous claims by Hallam *et al.*[9]

C. Permanent recovery of both fast and slow B-O related degradation

In this section, the permanent deactivation of B-O defects is considered, with an emphasis on lifetime recovery of the fast and slow degradation stages. Figure 6 shows lifetime curves at various stages of B-O related processing on samples without iron. Curves are shown after typical fast or slow degradation, and where the extent of fast degradation has been greatly enhanced using thermal annealing.[17] The lifetimes of the samples were sufficiently high to observe the first stage of degradation, as shown in our previous studies.[17,18] *FDD* by fast degradation (FDD_{fast}), which is after 300 s of light soaking ($FDD_{fast,a}$), was ≈75% on the sample with annealing at 200 °C for 15 s, while another sample with annealing at 200 °C for 600 s showed $FDD_{fast,b} \approx 15\%$. It should be noted that the 200 °C dark annealing process for 600 s represents the conventional dark annealing process used in many B-O defect studies including that performed by Bothe *et al.*[4,11,59–63] For clarity, curves are also shown in the dark annealed state (where B-O defects have been fully annihilated).

Lifetime curves are also shown after a permanent deactivation process was performed, as well as after a subsequent stability test. As is shown, almost identical lifetime curves

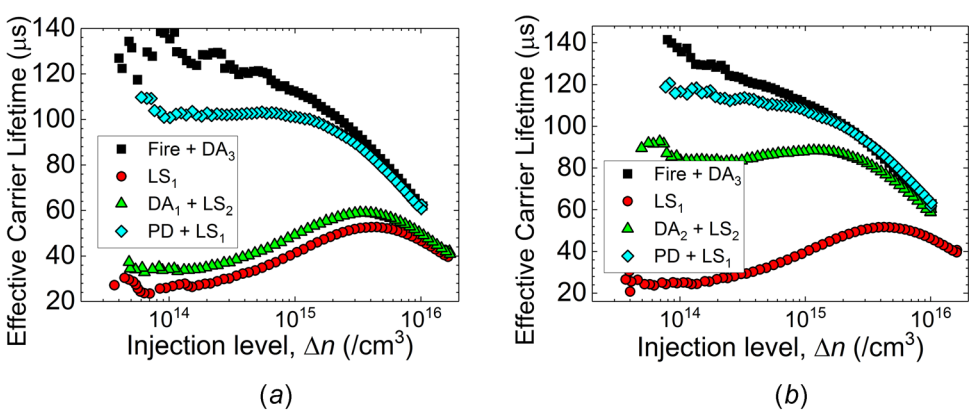

FIG. 6. Effective carrier lifetime curves of two samples with undetectable iron concentrations ($Fe_i < 0.1 \times 10^9/cm^3$) after firing at 596 °C and under dark annealing at 250 °C for 1 h (Fire + DA_3) (squares), light soaking for 48 h (LS_1) (circles), dark annealing at 200 °C (a) for 15 s with $FDD_{fast,a} \approx 75\%$ + light soaking for 300 s (DA_1 + LS_2) and (b) for 600 s with $FDD_{fast,b} \approx 15\%$ + light soaking for 300 s (DA_2 + LS_2) (triangles), and permanent deactivation under 1 sun illumination at 160 °C for 2 h + light soaking (PD + LS_1) (diamonds).

from two samples were obtained from that in the dark annealed state to that after the permanent recovery process and stability check. These curves were substantially higher than the lifetime curves after fast degradation, especially one with $FDD_{fast,a} \approx 75\%$ [see Fig. 6(a)]. The results demonstrate that the recombination activity of degradation that occurs in both fast and slow timescales can be passivated during the permanent recovery. The conventional method to dissociate B-O defect by dark annealing at 200 °C for 600 s is done in Fig. 6(b), which had $FDD_{fast,b} \approx 15\%$. The two results with different FDD_{fast} provide adequate evidence that the B-O defects can be fully passivated. It should be noted that these results greatly differ from those reported in a recent publication by Voronkov and Falster, suggesting that recombination activity related to rapid degradation cannot be permanently deactivated.[21]

When we performed the same test on an iron-contaminated sample, a high apparent k-value was obtained after a permanent deactivation process (see Fig. 7). The k-value after the complete permanent deactivation and stability test was compared with the k-value reported by Voronkov *et al.*[16] Although the k-value obtained with Fe-B pair dissociation after the permanent deactivation process (51 ± 8) was less than the k-value of 65 reported by Voronkov *et al.*,[16] it is in close agreement with the high apparent capture cross-section ratio reported after permanent deactivation.[21]

It should be noted that this value is substantially lower than a value of 286 assumed for Fe_i. This is likely due to the presence of other SRH recombinations, evident in the samples after dark annealing. Subsequent lifetime measurements were performed after leaving the samples in the dark at room temperature, which showed a k-value of close to 8, which also confirmed the characteristic cross-over behavior of iron in the samples before and after 5 s of light soaking under 1 sun after permanent deactivation and stability test ($PD + LS_1$ vs. $PD + LS_1 + LS_3$ in Fig. 7).

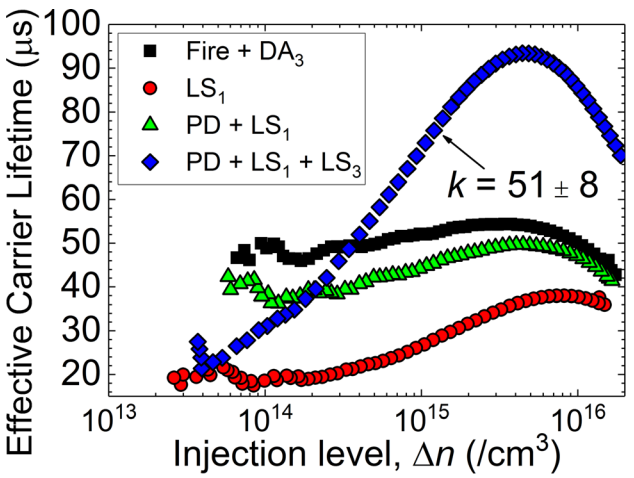

FIG. 7. Effective carrier lifetime curve of a sample with $[Fe_i] = 3.1 \pm 0.6 \times 10^{11}/cm^3$ after firing at 596 °C and dark annealing at 250 °C for 1 hour (Fire + DA_3) (squares), light soaking for 48 h (LS_1) (circles), permanent deactivation under 1 sun illumination at 160 °C for 2 h and stability test ($PD + LS_1$) (triangles), and after iron dissociation with 1 sun illumination at room temperature for 5 s ($PD + LS_1 + LS_3$) (diamonds).

Furthermore, this was only observed when Fe_i was present in the sample. Hence, we were able to permanently deactivate all B-O related recombinations, irrespective of the different percentages of FDD_{fast} shown previously in Fig. 6. This is in excellent agreement with the previous results shown by Wilking *et al.*[64] These results provide an alternative explanation to the previous suggestion that recombination in the fast timescale cannot be passivated.[21] They also suggest that iron is not effectively passivated during the permanent deactivation process, and as a result, the presence of Fe_i in a wafer can result in higher k-values after permanent deactivation.

D. Implication of the new findings for previous observations and models

Many B-O defect theories appear to have been developed based on the assumption of two independent defects due to the distinctively different kinetics and recombination properties that were previously observed.[11,16] However, this paper shows that those different behaviours can be adequately described by the known behaviour of iron in boron doped Cz silicon. The results in this work provide further evidence for the involvement of a single B-O defect, in contrast to earlier studies suggesting the involvement of two defects, namely the FRC and the SRC.[11,16] We also suggest that the recent thermal and illumination histories of the samples can have an impact on the subsequent meta-stable behaviour of B-O related defect studies. In particular, the prior processes can allow interstitial iron present in the sample to have a major impact on the observed kinetics.

The results in this work also have three important implications for the nature of the B-O defect. Firstly, the results lend further weight to a latent-centre based defect model described by Voronkov *et al.*[19] Within a latent centre model, the B-O defect is a chemically stable species involving boron and oxygen. B-O defect undergoes only configurational changes rather than chemical association/dissociation while transitioning between recombination inactive forms to the recombination active form. This is consistent with a number of studies that have ruled out the direct participation of B and O_{2i} during the degradation and annealing processes (see Voronkov *et al.*[19] for the explanation and references therein for an expanded discussion).

The second important implication is that the B-O defect is likely a single defect rather than two separate defects. Such a single defect model was previously described by the authors in Ref. 17, wherein the fully formed B-O defects have an immediate precursor, A_2, as well as a precursor to state A_2 termed A_1. The diagram of the single defect model is shown in Fig. 8. The figure does not include the permanently deactivated state,[53] which is commonly defined, as it is not the scope of the study.

Within such a model, the activation energy (E_a) associated with SRC formation, $E_{gen.slow}$ (0.475 eV), represents the activation energy of the transition $A_1 \rightarrow A_2$ ($E_{a,A1A2}$). $E_{gen.fast}$ (0.23 eV), the activation energy formerly associated with the FRC activation,[11] would therefore be the transition from A_2 to B ($E_{a,A2B}$). Note that state B is the only recombination

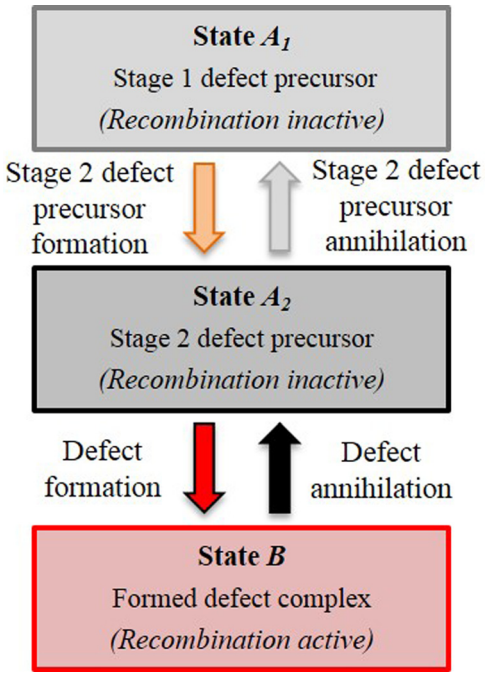

FIG. 8. Diagram of the B-O single defect model and the steps of B-O defect formation.

active configuration of the B-O defect, while states A_1 and A_2 are inactive. Thus, it can appear to be an additional stage in the formation of the B-O defects that is not directly detectable via lifetime spectroscopy due to both the start and end states of the transition being recombination inactive.

Previously within a latent centre framework, it was assumed that either two or three meta-stable configurations of the B-O latent centre exist,[19] which was related to either the annealed and degraded states (corresponding to states A_2 and B), or the annealed, degraded and regenerated states (corresponding to states A, B and C). However, a single defect model implies a fourth defect state, A_1, and could be interpreted in one of two ways within a latent centre framework. Either (a) state A_1 represents the dissociated precursors of the latent centre and is therefore not a mere configurational change, or (b) state A_1 represents a configurational change, leading to at least three metastable configurations for the B-O latent centre (corresponding to A_1, A_2 and B)—and possibly four, if C is also considered a configurational change.

However, the first hypothesis is unlikely for three reasons. Firstly, it is clear from recent work that thermal dissociation and formation of the latent centre most likely happen at temperatures above 450 °C.[44] In contrast, transitions involving states A_2, B and C are known to occur up to at least 300 °C in p-type silicon[3,11,17] and at least 250 °C in compensated n-type silicon. Thus, if A_1 represents the thermally dissociated state of the latent centre, transitions involving A_1 would be expected to occur at least above 300 °C and most likely above 450 °C. However, the transitions between A_1 and A_2 are shown in this and previous work[17] to occur at temperatures as low as 160 °C. This is also supported by a comparison of the associated activation energies. If an oxygen dimer based latent centre is assumed, the thermal formation of the latent centre is likely to be limited by the activation energy associated with oxygen diffusivity, resulting in an activation energy of 2.53 eV.[65] In contrast, the transitions $A_2 \rightarrow A_1$ and $A_1 \rightarrow A_2$ were shown in a previous work[17] to involve activation energies of ∼0.91 eV and ∼0.43 eV, respectively. Secondly, it must be noted that the activation energies associated with the known transitions between A_2, B and C are of the same magnitude (all less than 1.5 eV) as those involving A_1 and A_2. The similarity in activation energies may suggest that A_1 represents another configuration of the latent centre much like the states A_2 and B (possibly also C), rather than the thermally dissociated state. Finally, while it is possible that A_1 represents some other state unrelated to both thermal formation/dissociation as well as the latent centre, it must be noted that no such transition has ever been observed or found to be required to explain the known behaviour of the B-O defect.

Thus, the points above suggest that A_1 is another configuration of the B-O latent centre [case (b) described above]. This raises the question of whether A_1 as an additional configurational state of the latent centre is compatible with existing experimental observations. In this regard, the observed dependence of degradation kinetics on the electron concentration (at low illumination intensities)[3,66] and on the hole concentration (at higher illumination intensities)[67] reveals an important insight. Previously, it was assumed that degradation ($A_2 \rightarrow B$) involved both a charge state change (addition of an electron) and a configurational change (involving the capture of two holes). Since it is likely that A_1 transitions exclusively to A_2 and then to B rather than directly to B (any direct transitions between A_1 and B would be detectable by changes in the lifetime, but this was not observed in previous experiments[17]), it is possible that the charging transition involving an electron capture is in fact $A_1 \rightarrow A_2$, whereas the transition $A_1 \rightarrow B$ represents the configurational change involving hole capture. While further work is required to confirm this relation, it is possible that an additional configuration (A_1) is certainly plausible and could explain the known carrier dependence of the kinetics of B-O degradation.

IV. CONCLUSION

This paper highlights the importance of correctly accounting for other meta-stable defects and the sample history when studying B-O defects. In our sample, it demonstrates that the presence of interstitial iron could explain key behaviours from the literature that were previously used to establish B-O defect theories suggesting the existence of two separate B-O defects, namely the FRC and the SRC.[11,16,21] Subsequently, it provides further evidence to support the recent hypothesis that B-O degradation in Cz silicon is caused by a single defect.

In particular, three key B-O related behaviours published in the literature can be explained by the presence of iron. Firstly, Fe_i can account for the high reported k-values during the early stages of B-O degradation[11,16,19] that were previously attributed to the FRC. We show that in iron-contaminated samples, Fe-B dissociation during early stages of B-O related degradation can result in k_{app} values of

approximately 100, which decreases throughout the degradation process to 10. In contrast, iron free samples show a constant k_{app} value of approximately 10 (or 18, assuming a two-level defect) throughout degradation.

Secondly, the association to Fe-B pairs in the dark provides an alternative explanation for the initial recovery in a two-stage recovery of annihilation rate of FRC.[11] In iron-contaminated samples, the *NDD* that was extracted below the cross-over point showed an initial recovery in the first 100 s of dark annealing at 375 K. However, when the *NDD* was extracted at the cross-over point, no initial recovery was observed. Furthermore, in iron free samples, only a single stage of lifetime recovery was observed, which suggests that the initial recovery that was observed in previous studies was due to the association of Fe-B pairs, not a two stage recovery of B-O defects. Therefore, the injection level used to determine *NDD* is critical to consider, as samples with iron can be highly influenced by the meta-stable behaviour of Fe-B to illumination and temperature, which also influence B-O defects.

Thirdly, the B-O related recombination introduced in both the fast and slow timescales can be permanently deactivated. Despite the amount of FDD_{fast}, complete passivation of B-O defects was observed. Samples with iron showed drastically high k_{app} after the permanent deactivation process, which was previously interpreted as an incomplete passivation of the B-O defects formed by the fast degradation.[21] We conclude that the apparent existence of the SRC and the FRC was caused from a misinterpretation of data, where the results were affected by the presence of interstitial iron.

Hence, we show the B-O related degradation is caused by a single defect.

ACKNOWLEDGMENTS

The authors would like to acknowledge Kyung Kim, Ly Mai, Nino Borojevic, Hongzhao Li, and the MAiA processing team who assisted with wafer processing. This program has been supported by the Australian Government through the Australian Renewable Energy Agency (ARENA 1-A060) and the Australian Center for Advanced Photovoltaics (ARENA 1-SRI001). Brett Hallam would like to thank the Australian Research Council (ARC) for financial support through a Discovery Early Career Researcher Award (DE170100620). The views expressed herein are not necessarily the views of the Australian Government, and the Australian Government does not accept responsibility for any information or advice contained herein. The authors would like to thank the commercial partners of the ARENA 1-A060 project and the UK Institution of Engineering and Technology (IET) for their funding support for this work through the A.F. Harvey Engineering Prize.

[1]H. Fischer and W. Pschunder, "Investigation of photon and thermal induced change in silicon solar cells," in *Proceedings of the 10th IEEE Photovoltaic Specialists Conference* (1973), pp. 404–411.
[2]J. Schmidt and A. Cuevas, "Electronic properties of light-induced recombination centers in boron-doped Czochralski silicon," J. Appl. Phys. **86**(6), 3175–3180 (1999).
[3]J. Schmidt and K. Bothe, "Structure and transformation of the metastable boron- and oxygen-related defect center in crystalline silicon," Phys. Rev. B **69**(2), 24107 (2004).
[4]D. W. Palmer, K. Bothe, and J. Schmidt, "Kinetics of the electronically stimulated formation of a boron-oxygen complex in crystalline silicon," Phys. Rev. B **76**(3), 35210 (2007).
[5]J. Knobloch, S. W. Glunz, V. Henninger *et al.*, "21% efficient solar cells processed from Czochralski grown silicon," in *Proceedings of the 13th European Photovoltaic Solar Energy Conference* (1995), pp. 9–12.
[6]V. V. Voronkov, R. Falster, A. V. Batunina, D. Macdonald, K. Bothe, and J. Schmidt, "Lifetime degradation mechanism in boron-doped Czochralski silicon," Energy Procedia **3**, 46–50 (2011).
[7]V. V. Voronkov, R. Falster, K. Bothe, and B. Lim, "Light-induced lifetime degradation in boron-doped Czochralski silicon: Are oxygen dimers involved?," Energy Procedia **38**, 636–641 (2013).
[8]V. Voronkov and R. Falster, "The nature of boron-oxygen lifetime-degrading centres in silicon," Phys. Status Solidi **13**(10–12), 712–717 (2016).
[9]B. Hallam, M. Abbott, T. Nærland, and S. Wenham, "Fast and slow lifetime degradation in boron-doped Czochralski silicon described by a single defect," Phys. Status Solidi - RRL **10**(7), 520–524 (2016).
[10]H. Hashigami, M. Dhamrin, and T. Saitoh, "Characterization of the initial rapid decay on light-induced carrier lifetime and cell performance degradation of Czochralski-grown silicon," Jpn. J. Appl. Phys., Part 1 **42**(5A), 2564–2568 (2003).
[11]K. Bothe and J. Schmidt, "Electronically activated boron-oxygen-related recombination centers in crystalline silicon," J. Appl. Phys. **99**(1), 13701 (2006).
[12]T. Niewelt, J. Schön, J. Broisch, W. Warta, and M. Schubert, "Electrical characterization of the slow boron oxygen defect component in Czochralski silicon," Phys. Status Solidi - RRL **9**(12), 692–696 (2015).
[13]F. E. Rougieux, B. Lim, J. Schmidt, M. Forster, D. MacDonald, and A. Cuevas, "Influence of net doping, excess carrier density and annealing on the boron oxygen related defect density in compensated n-type silicon," J. Appl. Phys. **110**(6), 063708 (2011).
[14]J. Schön, T. Niewelt, J. Broisch, W. Warta, and M. C. Schubert, "Characterization and modelling of the boron-oxygen defect activation in compensated n-type silicon," J. Appl. Phys. **118**(24), 245702 (2015).
[15]T. Niewelt, J. Schon, W. Warta, S. W. Glunz, and M. C. Schubert, "Degradation of crystalline silicon due to boron–oxygen defects," IEEE J. Photovoltaics **7**(1), 383–398 (2017).
[16]V. V. Voronkov, R. Falster, K. Bothe, B. Lim, and J. Schmidt, "Lifetime-degrading boron-oxygen centres in p-type and n-type compensated silicon," J. Appl. Phys. **110**(6), 63515 (2011).
[17]M. Kim, M. Abbott, N. Nampalli, S. Wenham, B. Stefani, and B. Hallam, "Modulating the extent of fast and slow boron-oxygen related degradation in Czochralski silicon by thermal annealing: Evidence of a single defect," J. Appl. Phys. **121**, 53106 (2017).
[18]B. Hallam, M. Kim, M. Abbott *et al.*, "Recent insights into boron-oxygen related degradation: Evidence of a single defect," Sol. Energy Mater. Sol. Cells **173**, 25–32 (2017).
[19]V. V. Voronkov and R. Falster, "Light-induced boron-oxygen recombination centres in silicon: Understanding their formation and elimination," Solid State Phenom. **205**, 3–14 (2014).
[20]V. V. Voronkov, R. Falster, B. Lim, and J. Schmidt, "Boron-oxygen related lifetime degradation in p-type and n-type silicon," ECS Trans. **50**(5), 123–136 (2013).
[21]V. V. Voronkov and R. Falster, "Permanent deactivation of boron-oxygen recombination centres in silicon," Phys. Status Solidi **253**(9), 1721–1728 (2016).
[22]J. D. Murphy, K. Bothe, R. Krain, V. V. Voronkov, and R. J. Falster, "Parameterisation of injection-dependent lifetime measurements in semiconductors in terms of Shockley-Read-Hall statistics: An application to oxide precipitates in silicon," J. Appl. Phys. **111**(11), 113709 (2012).
[23]T. Niewelt, S. Mägdefessel, and M. C. Schubert, "Fast *in-situ* photoluminescence analysis for a recombination parameterization of the fast BO defect component in silicon," J. Appl. Phys. **120**(8), 85705 (2016).
[24]N. Nampalli, T. H. Fung, S. Wenham, B. Hallam, and M. Abbott, "Statistical analysis of recombination properties of the boron-oxygen defect in p-type Czochralski silicon," Front. Energy **11**(1), 4–22 (2017).
[25]D. Macdonald, A. Cuevas, and J. Wong-Leung, "Capture cross sections of the acceptor level of iron–boron pairs in p-type silicon by injection-level dependent lifetime measurements," J. Appl. Phys. **89**(12), 7932–7939 (2001).

[26]L. J. Geerligs and D. Macdonald, "Dynamics of light-induced FeB pair dissociation in crystalline silicon," Appl. Phys. Lett. **85**(22), 5227–5229 (2004).
[27]J. Schmidt, "Effect of dissociation of iron-boron Pairs in crystalline silicon on solar cell properties," Prog. Photovoltaics **13**(4), 325–331 (2005).
[28]D. MacDonald, T. Roth, P. N. K. Deenapanray, T. Trupke, and R. A. Bardos, "Doping dependence of the carrier lifetime crossover point upon dissociation of iron-boron pairs in crystalline silicon," Appl. Phys. Lett. **89**(14), 142107 (2006).
[29]H. Li, K. Kim, B. Hallam, B. Hoex, S. Wenham, and M. Abbott, "$POCl_3$ diffusion for industrial Si solar cell emitter formation," Front. Energy **11**(1), 42–51 (2017).
[30]H. Li, B. Hallam, S. Wenham, and M. Abbott, "Oxidation drive-in to improve industrial emitter performance by $POCl_3$ diffusion," IEEE J Photovoltaics **7**(1), 144–152 (2017).
[31]A. Y. Liu and D. Macdonald, "Precipitation of iron in multicrystalline silicon during annealing," J. Appl. Phys. **115**(11), 114901 (2014).
[32]M. Kim, P. Hamer, H. Li *et al*., "Impact of thermal processes on multicrystalline silicon," Front. Energy **11**(1), 32–41 (2017).
[33]T. Buonassisi, A. A. Istratov, S. Peters *et al*., "Impact of metal silicide precipitate dissolution during rapid thermal processing of multicrystalline silicon solar cells," Appl. Phys. Lett. **87**(12), 121918 (2005).
[34]B. Hallam, D. Chen, M. Kim *et al*., "The role of hydrogenation and gettering in enhancing the efficiency of next generation Si solar cells: An industrial perspective," Phys. Status Solidi **214**(7), 1700305 (2017).
[35]Z. Hameiri, N. Borojevic, L. Mai, N. Nandakumar, K. Kim, and S. Winderbaum, "Thermally stable and low-absorbing industrial silicon nitride films with very low surface recombination," IEEE J Photovoltaics **7**, 996–1003 (2017).
[36]S. Rein and S. W. Glunz, "Electronic properties of interstitial iron and iron-boron pairs determined by means of advanced lifetime spectroscopy," J. Appl. Phys. **98**, 113711 (2005).
[37]R. A. Sinton and A. Cuevas, "Contactless determination of current–voltage characteristics and minority-carrier lifetimes in semiconductors from quasi-steady-state photoconductance data," Appl. Phys. Lett. **69**(17), 2510–2512 (1996).
[38]H. Nagel, C. Berge, and A. G. Aberle, "Generalized analysis of quasi-steady-state and quasi-transient measurements of carrier lifetimes in semiconductors," J. Appl. Phys. **86**(11), 6218 (1999).
[39]A. Richter, F. Werner, A. Cuevas, J. Schmidt, and S. W. Glunz, "Improved parameterization of Auger recombination in silicon," Energy Procedia **27**, 88–94 (2012).
[40]D. H. Macdonald, L. J. Geerligs, and A. Azzizi, "Iron detection in crystalline silicon by carrier lifetime measurements for arbitrary injection and doping," J. Appl. Phys. **95**(3), 1021–1028 (2004).
[41]R. A. Sinton and R. M. Swanson, "Recombination in highly injected silicon," IEEE Trans. Electron Devices **34**(6), 1380–1389 (1987).
[42]J. M. Dorkel and P. Leturcq, "Carrier mobilities in silicon semi-empirically related to temperature, doping and injection level," Solid State Electron. **24**(9), 821–825 (1981).
[43]N. Nampalli, H. Li, M. Kim *et al*., "Multiple pathways for permanent deactivation of boron-oxygen defects in p-type silicon," Sol. Energy Mater. Sol. Cells **173**, 12–17 (2017).
[44]D. C. Walter, R. Falster, V. V. Voronkov, and J. Schmidt, "On the equilibrium concentration of boron-oxygen defects in crystalline silicon," Sol. Energy Mater. Sol. Cells **173**, 33–36 (2017).
[45]D. Macdonald, T. Rothprakash, P. N. Deenapanraykarsten, K. Bothe, P. Pohl, and J. Schmidt, "Formation rates of iron-acceptor pairs in crystalline silicon," J. Appl. Phys. **98**(8), 83509 (2005).
[46]J. Lindroos and H. Savin, "Review of light-induced degradation in crystalline silicon solar cells," Sol. Energy Mater. Sol. Cells **147**, 115–126 (2016).
[47]H. Savin, M. Yli-Koski, and A. Haarahiltunen, "Role of copper in light induced minority-carrier lifetime degradation of silicon," Appl. Phys. Lett. **95**(15), 152111 (2009).
[48]D. Chen, M. Kim, B. V. Stefani *et al*., "Evidence of an identical firing-activated carrier-induced defect in monocrystalline and multicrystalline silicon," Sol. Energy Mater. Sol. Cells. **172**, 293 (2017).
[49]T. Niewelt, J. Schön, J. Broisch, S. Mägdefessel, W. Warta, and M. C. Schubert, "A unified parameterization for the formation of boron oxygen defects and their electrical activity," Energy Procedia **92**, 170–179 (2016).
[50]J. D. Murphy, K. Bothe, R. Krain, V. V. Voronkov, and R. J. Falster, "The impact of oxide precipitates on minority carrier lifetime in Czochralski silicon," ECS Trans. **50**(5), 137–144 (2013).
[51]D. Macdonald, A. Cuevas, A. Kinomura, and Y. Nakano, "Phosphorus gettering in multicrystalline silicon studied by neutron activation analysis," in 29th IEEE PVSC (2002), pp. 285–288.
[52]K. Bothe, R. Hezel, and J. Schmidt, "Understanding and reducing the boron-oxygen-related performance degradation in Czochralski silicon solar cells," Solid State Phenom. **95–96**(i), 223–228 (2004).
[53]A. Herguth, G. Schubert, M. Kaes, and G. Hahn, "A new approach to prevent the negative impact of the metastable defect in boron doped Cz silicon solar cells," in *Proceedings of the 4th IEEE World Conference on Photovoltaic Energy Conversion (2006)*, pp. 940–943.
[54]S. Wilking, C. Beckh, S. Ebert, A. Herguth, and G. Hahn, "Influence of bound hydrogen states on BO-regeneration kinetics and consequences for high-speed regeneration processes," Sol. Energy Mater. Sol. Cells **131**, 2–8 (2014).
[55]S. M. Kim, S. Chun, S. Bae *et al*., "Light-induced degradation and metastable-state recovery with reaction kinetics modeling in boron-doped Czochralski silicon solar cells," Appl. Phys. Lett. **105**(8), 83509 (2014).
[56]A. Herguth, G. Schubert, M. Kaes, and G. Hahn, "Avoiding boron-oxygen related degradation in highly boron doped Cz silicon," in *Proceedings of the 21st European Photovoltaic Solar Energy Conference (2006)*, pp. 530–537.
[57]H. Hieslmair, "Time constants of degradation, regeneration, and destabilization of the BO related defect," in *2016 43rd IEEE Photovoltaics Specialists Conference (PVSC)* (2016), pp. 0645–0650.
[58]M. Kim, D. Chen, M. Abbott, S. Wenham, and B. Hallam, "Investigating the influence of interstitial iron on the study of boron-oxygen defects," in *33rd European Photovoltaic Solar Energy Conference and Exhibition* (2017), pp. 328–332.
[59]B. Lim, K. Bothe, and J. Schmidt, "Deactivation of the boron–oxygen recombination center in silicon by illumination at elevated temperature," Phys. Status Solidi-RRL **2**(3), 93–95 (2008).
[60]B. Lim, F. Rougieux, D. Macdonald *et al*., "Generation and annihilation of boron–oxygen-related recombination centers in compensated p-and n-type silicon," J. Appl. Phys. **108**(10), 103722 (2010).
[61]K. Bothe, R. Hezel, and J. Schmidt, "Recombination-enhanced formation of the metastable boron–oxygen complex in crystalline silicon," Appl. Phys. Lett. **83**(6), 1125–1127 (2003).
[62]C. Möller and K. Lauer, "Light-induced degradation in indium-doped silicon," Phys. Status Solidi - RRL **7**(7), 461–464 (2013).
[63]K. Bothe, J. Schmidt, and R. Hezel, "Effective reduction of the metastable defect concentration in boron-doped Czochralski silicon for solar cells," in *Proceedings of the 29th IEEE Photovoltaic Specialists Conference (2002)*, pp. 194–197.
[64]S. Wilking, M. Forster, A. Herguth, and G. Hahn, "From simulation to experiment: Understanding BO-regeneration kinetics," Sol. Energy Mater. Sol. Cells **142**, 87–91 (2015).
[65]R. C. Newman, "Oxygen diffusion and precipitation in Czochralski silicon," J. Phys.: Condens. Matter **12**(25), R335 (2000).
[66]H. Hashigami, Y. Itakura, and T. Saitoh, "Effect of illumination conditions on Czochralski-grown silicon solar cell degradation," J. Appl. Phys. **93**(7), 4240–4245 (2003).
[67]P. Hamer, N. Nampalli, Z. Hameiri *et al*., "Boron-oxygen defect formation rates and activity at elevated temperatures," Energy Procedia **92**, 791–800 (2016).